Jovan Stepanovic,
Dragan Stojiljkovic,
***Ineta Vilumsone-Nemes,**
****Petar Mitkovic**

Modelling the Strength-Elongation Characteristic of Forming Fabrics for the Paper Industry

University of Nis,
Faculty of Technology
Niš, Serbia

***University of Novi Sad,**
Technical Faculty
Novi Sad, Serbia,

****University of Nis,**
Faculty of Civil Engineering and Architecture
Niš, Serbia

E-mail: jovan@tf.ni.ac.rs

Abstract
The mechanical properties of SSB (Sheet Support Binder) forming fabrics depend on their structural solutions. A particular problem of the structures formed is their lower strength in the binder area. Analysed were binders for three types of multilayer fabrics with the same yarn composition but with different yarn densities and weaves. The test was performed on a Zwick dynamometer supported by TextXpert V.11.0 software. Based on the results obtained force-elongation relations were formed, the creep limits of the binder defined, and rheological models developed that can be used to simulate the behaviour of SSB forming fabrics in the binder area during the operation.

Key words: *forming fabrics, weave, breaking load, elongation at break, creeping, rheological model.*

Introduction

Forming fabrics are used in the paper industry, playing a very important role in the formation of a sheet of paper. These functions can be divided into two main groups: technological (the ability to retain fibres, oriented transport and deposition of fibres on the surface of the fabric, and water permeability) and mechanical (abrasion resistance, stain resistance and stability of the fabric) [1 - 3].

The conditions for the formation of SSB fabric (Sheet Support Binder) with good mechanical properties are generated using appropriate yarn. However, the biggest problem is the behaviour of the fabric in the joint area. Modern solutions for joint forming by the weaving technique allow correct structural solutions in the area of the joint, which are reflected in SSB fabrics of equal thickness and weave. However, these parts of the fabrics have a lower breaking load by about 50% [4], which causes the deformation of the fabric during operation and adversely affects the durability of the fabric. Therefore this paper presents a method of determining the load of SSB forming fabric allowed (in the joint area) during operation. In addition, a suitable rheological model is selected which describes the behaviour of the SSB fabric formed in the joint area in terms of the effects of the tensile force. This generated conditions for simulation of the behaviour of the SSB fabric in the joint area during operation, contributing to the correct prediction of the intensity of the tensile force which the SSB fabric in the joint area can withstand during operation without deforming.

Theoretical considerations

To simulate the behaviour of SSB forming fabric, it is necessary to establish the relationship between the load acting on the SSB fabric and the deformation thereof at the same time. For describing the behavior of SSB forming fabric differential equations are established, obtained on the basis of mechanical models. Thus each type of deformation of real materials is imitated by a simple model or that imitation is represented by complex models formed by a combination of simple models [5, 6].

The simple models used to describe elastic, viscoelastic and plastic deformations define the properties of ideal materials not found in nature, simply approximating the behaviour of real materials under certain load conditions and other external influences.

The rheological model for ideal elastic material is the elastic spring (Hooke spring). This material subjected to a uniaxial load acts in accordance with Hooke's law. The rheological model for viscose material is a piston which moves in oil (Newton's body). As the real material, more or less, always contains elements of these models, it is necessary to come up with another type of material referred to as viscoelastic material, which at the same time under a load shows properties of elastic bodies and viscous liquids, meaning that their strain depends on the size speed of deformation.

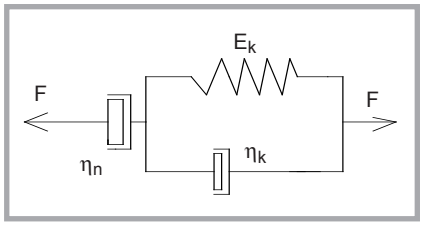

Figure 1. *Leserič model.*

By combining the basic rheological models, a Leserič body rheological model is established (***Figure 1***).

The Leserič body (L) represents a serial link between Newton (N) and Kelvin (*K*) models [7]:

$$L = N - - - K$$

The deformation rate of the Leserič body is equal to the sum of those of the Newton and Kelvin bodies:

$$\dot{\varepsilon}_L = \dot{\varepsilon}_N + \dot{\varepsilon}_K$$

where: $\dot{\varepsilon}_N$ is the deformation rate of the Newton body, $\dot{\varepsilon}_K$ is the deformation rate of the Kelvin body.

The deformation rate of the Newton body is equal to:

$$\dot{\varepsilon}_N = \frac{\sigma}{\eta_N}$$

where: η_N is the Newton body's viscosity coefficient.

The deformation rate of the Kelvin model is equal to:

$$\dot{\varepsilon}_K = \frac{\sigma}{\eta_K} - \frac{E_K}{\eta_K} \cdot \varepsilon_K$$

where: E_K is the elasticity module of the Kelvin model, η_K is the viscosity coefficient of the Kelvin model.

Stepanovic J, Stojiljkovic D, Vilumsone-Nemes I, Mitkovic P. Modelling the Strength-Elongation Characteristic of Forming Fabrics for the Paper Industry. *FIBRES & TEXTILES in Eastern Europe* 2014; 22, 4(106): 112-116.

After some mathematical operations the following expression is obtained for the rate of deformation of the Leserič body:

$$\dot{\varepsilon} = \frac{\sigma}{\eta_N} + \frac{\sigma}{\eta_k} - \frac{E_K}{\eta_K} \cdot \exp\left(-\frac{E_K}{\eta_K} \cdot t\right) \cdot \left[\varepsilon_o + \frac{1}{\eta_K} \cdot \int \sigma \cdot \exp\left(\frac{E_K}{\eta_K} \cdot t\right) dt\right]$$

where: ε_0 is the initial relative elongation.

Differentiation by the time and rearrangement of the previous expression gives a differential equation of the rheological model in the following form:

$$\ddot{\varepsilon} \cdot \eta_K + \dot{\varepsilon} \cdot E_K \cdot \eta_K = \dot{\sigma}(\eta_N + \eta_K) + \sigma \cdot E_K$$

As $\dot{\varepsilon} = const$ and $\varepsilon = 0$, this differential equation can be represented in the form:

$$\sigma = -C \cdot \exp\left(-\frac{E_K}{\eta_K + \eta_N} \cdot t\right) + \eta_N \cdot \dot{\sigma}$$

The integration constant, C, is determined from the initial conditions t = 0, σ = 0. The voltage-time dependence, after determining the integration constant, has the form:

$$\sigma = \eta_N \cdot \dot{\sigma} \cdot \left[1 - \exp\left(\frac{t}{\tau_r}\right)\right]$$

where: $\tau_r = (\eta_N + \eta_K)/E_K$ relaxation time. The stress-elongation dependence has the form:

$$\sigma = \eta_N \cdot \dot{\sigma} \cdot \left[1 - \exp\left(\frac{l_o}{100 \cdot v \cdot \tau_r} \cdot \varepsilon\right)\right]$$

where: l_o - starting test tube's length, v – test speed

Materials and methods

All three forming SSBs have a commercial application. SSB fabric 1V1P41 (***Figure 2***) is formed on a weaving machine as double fabric joined by special binding weft wires (01, 02). The fabric has an upper warp (02, 04, ..., 20) which binds to the upper weft (04) in the plain weave. The lower warp (01, 03, ..., 19) binds with the lower weft (03) in a five-wire satin weave. The binder weft is two times denser (the number of wires in cm) in regard to the warp of the upper fabric. At the same time it alternately binds with the upper warp in plain weave and with the lower warp in an irregular ten-wire satin weave.

SSB fabric 1V1P51 (***Figure 3***) is formed on a weaving machine as double fabric joined with special binding weft wires (01, 02). The fabric has an upper warp (2, 4, ..., 24) which binds with the upper weft in a plain weave (04). The lower warp (1, 3, ..., 23) binds with the lower weft (03) in a six-wire satin weave. The binding weft has the same density as the weft of the upper fabric. At the same time it alternately binds with the upper warp in plain weave and with the lower warp in an irregular twelve-wire satin weave.

SSB fabric 1V2P51 (***Figure 4***) is formed on a weaving machine as double fabric joined with special binding weft wires (1, 2). The fabric has an upper warp (2, 4, ..., 24) which binds with the upper weft in plain weave (4 and 6). The lower warp (1, 3, ..., 23) binds with the lower weft (3 and 5) in a six-wire satin weave. The binding weft has the same density as the weft of the upper fabric. At the same time it alternately binds with the upper warp in plain weave and with the lower warp in an irregular twelve-wire satin weave (Binder weft and weft of the upper fabric bind in a proportion of 2:2).

Tables 1 and ***2*** (see page 114) contain the characteristics of the monofilament yarns and warp and weft densities of the SSB fabrics applied.

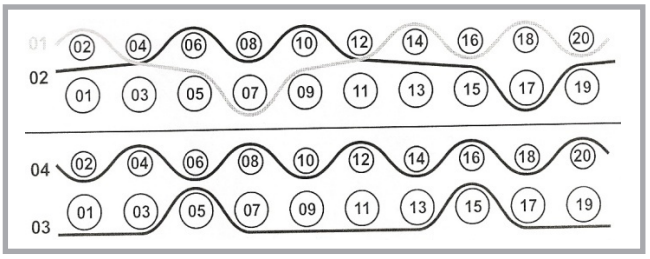

Figure 2. *1V1P41 binder cross section.*

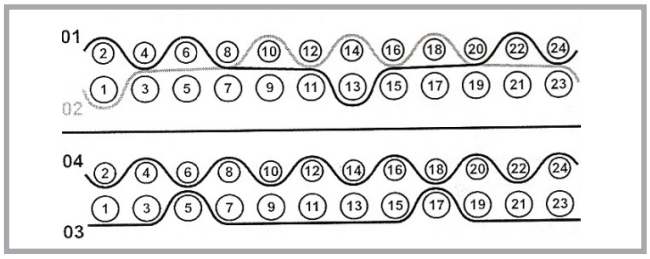

Figure 3. *1V1P51 binder cross section.*

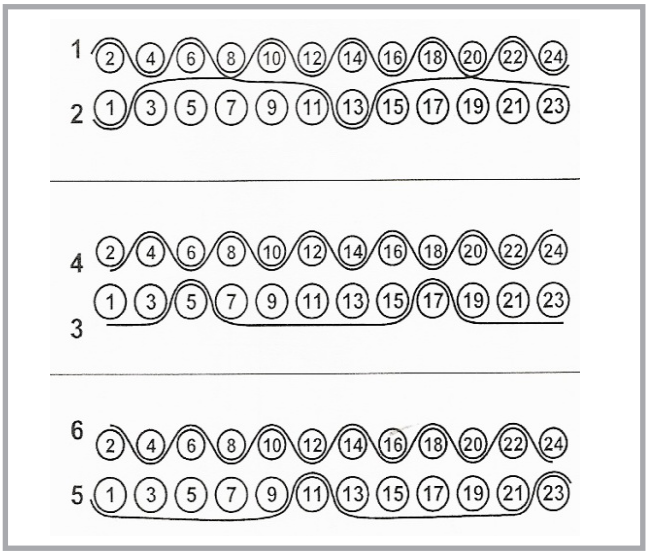

Figure 4. *1V2P51 binder cross section.*

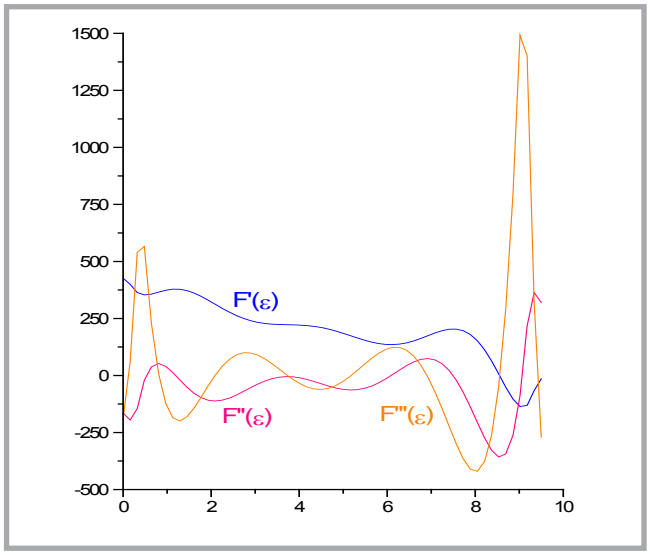

Figure 5. *First, second and third derivatives of function F (ε).*

Table 1. Monofilament yarn characteristics.

Position	Composition	Diameter, mm	Linear density, dtex	Breaking load, cN/tex	Elongation at break, %
Upper warp	PES	0.13	185	55.4	18.1
Lower warp		0.21	479	61.6	10.9
Upper weft		0.14	214	42.9	24.9
Lower weft		0.25	679	45.3	24.9
Lower weft	PA 6.6	0.25	562	55.2	45.7
Binding weft		0.13	152	63.9	37.7

Table 2. Warp and weft densities (number of wires in 1 cm) – [cm^{-1}]

Position	Composition	1V1P41, cm^{-1}	1V1P51, cm^{-1}	1V2P51, cm^{-1}
Upper warp	PES	30.5	30	30.5
Lower warp		30.5	30	30.5
Upper weft		19.5	21.5	23.5
Lower weft		9.75	10.75	11.75
Lower weft	PA 6.6	9.75	10.75	11.75
Binding weft		39.0	21.5	23.5

Testing of the tensile strength and elongation at break of the binders in the weft direction was performed on a Zwick dynamometer. Dimensions of the strips were 350 × 50 mm and after tearing the measuring width was 40 mm. The distance between the clamps was 200 mm.

The experiments were carried out under the following conditions:

- Pre-load force - 10 N
- Pre load speed - 20 mm/min
- Test speed - 80 mm/min.

In addition, based on the curve F - ε, the values of forces and relative elongation were determined at the creeping limit in the binder area (F_{cr}), whereby the first permanent deformation was generated, which occurs beyond the elasticity limit. It is determined numerically at the point of the local minimum of the second derivative of the curve F - ε, where $F'''(\varepsilon) = 0$ [8, 9] (***Figure 5***, binder 1V1P41). These data can be used to predict the limit load that the binders can handle without deformation.

Results and discussion

Investigation results of the breaking load and elongation at break testing for thermo stable SSB fabrics (thermal stabilisation provides length and width stability of the SSB fabric) are shown in ***Table 3***, and those of the investigation of the breaking load, elongation at break, creeping limit forces and creeping elongation in the region of joints are given in ***Table 4***.

The breaking characteristics of 1V1P41 fabric in the joint area are lower than those of thermo-stable fabric, where the reduction in the breaking load is 48.13%, and elongation at break - 49.41%. The reduction in the tensile force in the area of the joint of 1V1P51 fabric is 60.33% and in elongation- 64.36%. In 1V2P51 fabric, the breaking load in the joint area is lower by 49.35% and elongation at break by 51.24% compared to thermo-stable fabrics.

Table 3. Breaking load and elongation at break of thermo stable SSB fabrics.

	1V1P41		1V1P51		1V2P51	
	F_{max}, N	ε_{max}, %	F_{max}, N	ε_{max}, %	F_{max}, N	ε_{max}, %
X	3976	17.81	3786	18.07	3908	19.36
S	127.4	1.12	23.6	0.45	67.7	0.95
Cv	3.2	6.29	0.62	2.29	1.73	4.91

Table 4. Mechanical characteristics of joints.

	1V1P41				1V1P51				1V2P51			
	F_{max}, N	ε_{max}, %	F_{cr}, N	ε_{cr}, %	F_{max}, N	ε_{max}, %	F_{cr}, N	ε_{cr}, %	F_{max}, N	ε_{max}, %	F_{cr}, N	ε_{cr}, %
X	2063	9.01			1502	6.44			1979	9.44		
S	74.8	0.37	744	2.01	72.8	0.42	338	0.78	94.9	0.81	362	0.85
Cv	3.63	4.11			4.85	6.52			4.79	8.58		

The percentage of the reduced breaking load p_b and elongation p_ε in the joint area is determined by the ***Equation***:

$$p_b = \frac{F_b - F_{bj}}{F_b} \cdot 100\ ,\ \%$$

$$p_\varepsilon = \frac{\varepsilon_b - \varepsilon_{bj}}{\varepsilon_b} \cdot 100\ ,\ \%$$

where: F_b - breaking load of SSB fabric, F_{bj} - breaking load of SSB fabric in the joint area, ε_b - elongation at break of SSB fabric, ε_{bj} - elongation at break of SSB fabric in the joint area.

In 1V1P41 fabric the joint area may be subjected to a strain of up to 744 N without suffering the first permanent deformation, while the intensity of force of the first permanent deformation in the other two fabrics in the joint area is much lower. The value of forces at the creeping limit of 1V1P41 fabric is 18.71% compared to the breaking load of thermo-stable fabric, and 36.07% compared to the breaking load of the fabric in the joint area.

Based on the results obtained, it can be concluded that the properties of SSB fabric depend on the mechanical properties of the yarns for warp and weft applied, then the density of warp and weft wires and finally on the weave (construction) of the SSB forming fabric. For 1V1P41 fabric, which shows the best mechanical properties, the reverse side is a five-end satin weave (***Figure 2***), unlike fabrics 1V1P51 and 1V2P51, where it is of a six-end satin weave (***Figures 3*** and ***4***). The quotient of the number of variations and weave repeat [10] is more favorable for five-end satin, which, among other things, is the reason for the results obtained. In addition to the more suitable weave of the lower fabric, SSB 1V1P41 has a greater density of binding weft wires, which also contributes to the improved mechanical properties of the SSB fabric, compared to the other two analyses of SSB fabrics. SSB fabric 1V2P51 has better mechanical properties in comparison to SSB fabric 1V1P51,which is a result of the greater density of warp and weft wires of SSB 1V2P51 compared to SSB 1V1P51.

Figure 6 shows the measured and calculated values of $F(\varepsilon)$ and the relative error of the model for fabric 1V1P41 in the joint area.

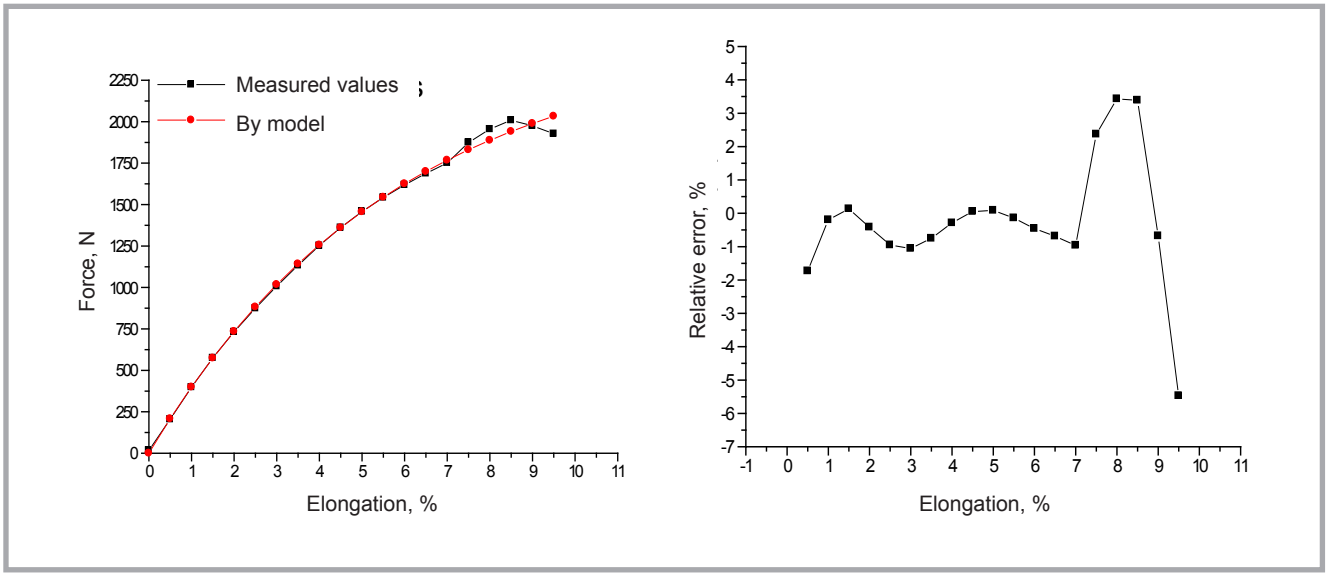

Figure 6. *Values of F(ε) measured and calculated (a) and relative error (b) for 1V1P41 fabric in the joint area according to Leserič model.*

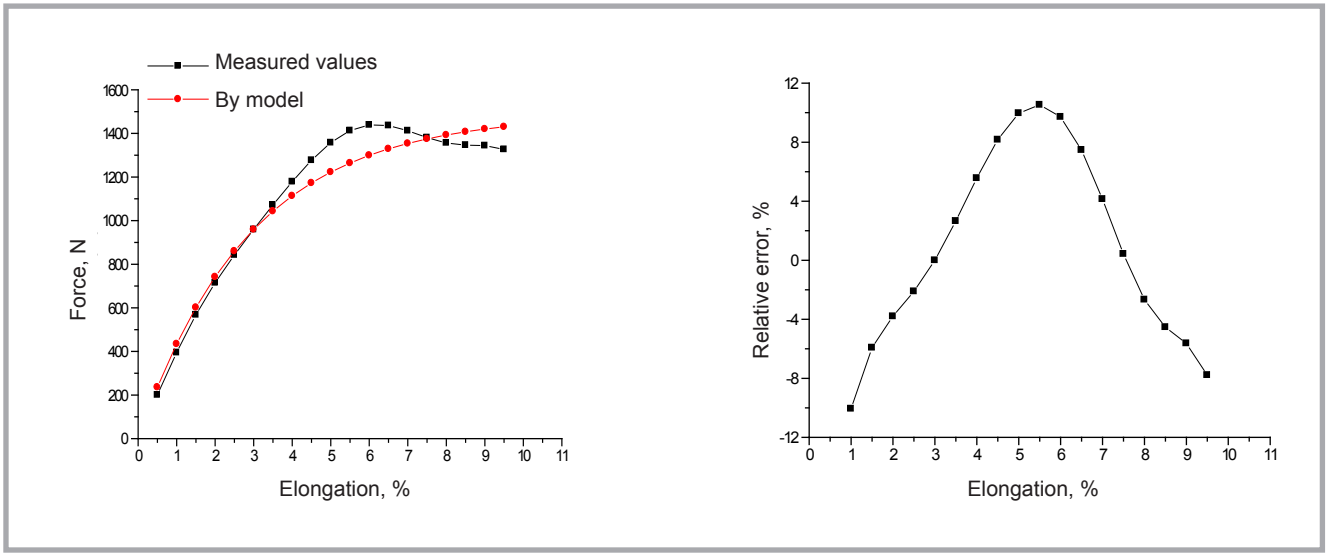

Figure 7. *Values of F(ε) measured and calculated (a) and relative error (b) for 1V1P51 fabric in the joint area according to Leserič model.*

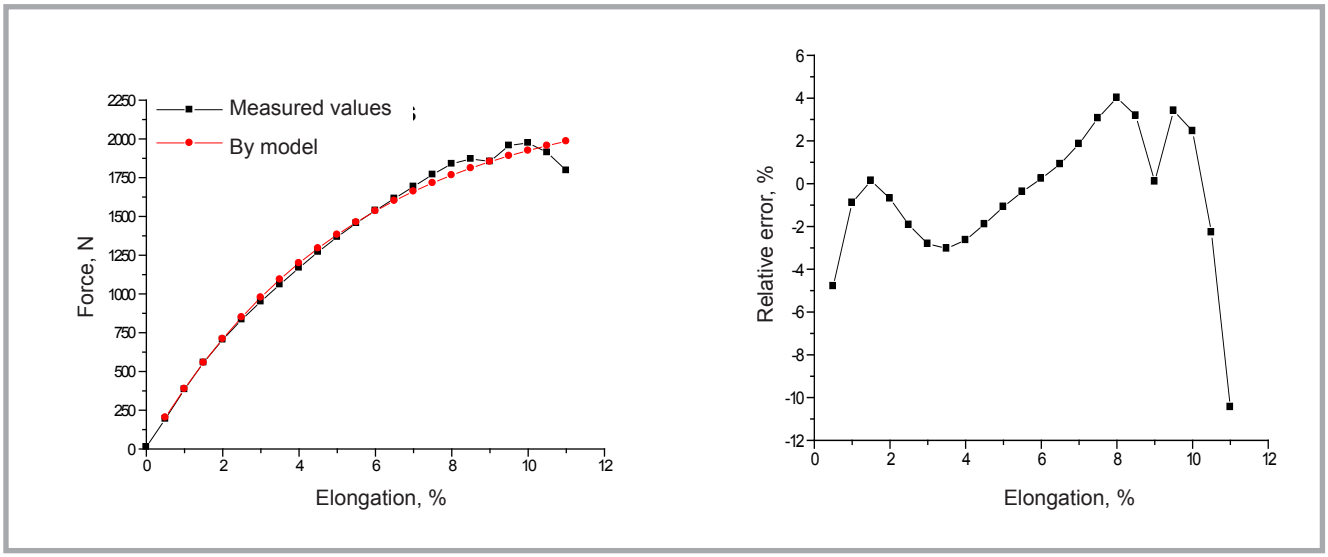

Figure 8. *Values of F(ε) measured and calculated (a) and relative error (b) for 1V2P51 fabric in the joint area according to the Leserič model.*

Table 5. *Model coefficients.*

1V1P41		1V1P51		1V2P51	
a	***b***	***a***	***b***	***a***	***b***
2528	0.17	1486	0.35	2275	0.19

Table 6. *Young's modulus and coefficient of dynamic viscosity.*

1V1P41		1V1P51		1V2P51	
E	***η***	***E***	***η***	***E***	***η***
867,600	1,945,000	1,028,000	1,143,000	851,000	1,750,000

In ***Figure 7***, given are the measured and calculated values of $F(\varepsilon)$ and the relative error of the model for 1V1P51 fabric in the joint area.

Figure 8 shows the measured and calculated values of $F(\varepsilon)$ and the relative error of the model for fabric 1V2P51 in the joint area.

Based on the experimental data and relation obtained by approximation from the rheological model, the following Equation was obtained:

$$\sigma = a\,(1 - e^{-b\cdot\varepsilon})$$

Model coefficients '*a*' and '*b*' are given in ***Table 5***.

Relation between coefficients "*a*" and "*b*" and physical characteristics are given in expressions:

$$E = 2000\,a\,b \text{ and } \eta = a/v$$

where: E - Young's modulus in N/m^2, η - coefficient of dynamic viscosity in Ns^2/m, v - speed of clamp during testing in m/s.

Equation $\sigma = a\,(1 - e^{-b\cdot\varepsilon})$ can be written in the form:

$$\sigma = \eta \cdot v\left(1 - e^{-\frac{E}{2000\cdot\eta\cdot v}\cdot\varepsilon}\right).$$

Table 6 shows the values of Young's module of elasticity and the coefficient of dynamic viscosity obtained based on the rheological model which was established by experimental data.

Analysing the relative error of the model, it can be confirmed that the maximum relative deviation of actual values from the theoretical is negligent. Thus it can be concluded that the model correctly describes the rheological behaviour of SSB fabric in the joint area when subjected to elongation. Also it can be concluded that the model describes the behaviour of the material up to the creeping limit very well, which is particularly important for the development of design methods for SSB fabrics in the area of the joint.

Conclusions

The mechanical properties of SSB forming fabric depend on the mechanical properties of the yarns for the warp and weft applied, then the density of warp and weft wires, and finally on the weaves (constructions) of the SSB. SSB fabrics of the same composition (warp PES, weft PES and PA, weft binder PA) were analysed, but of different wire density and weave.

On the basis of research results, it is concluded that forming SSB fabrics with applied five-wire satin weave on the reverse side of the fabric should take precedence over SSB fabrics with a six-wire satin weave applied. Also SSB fabrics have better mechanical properties with greater densities of warp and weft wires applied. The mechanical properties of all three types of fabrics deteriorate after the completion of joints, which indicates that the research should continue to find optimal solutions regarding the structure and design of SSB fabrics in the area of the joint.

Based on the results obtained a rheological model is developed that can be used to simulate the behaviour of SSB fabrics in the area of the joint during operation. Also it can be concluded that the model correctly describes the behaviour of the material up to the fabric's creeping limit in the region of the joint.

References

1. Dasgupta S, Ray N. Designing of Forming Fabrics considering paper making aspects *IPPTA Journal* 2009; 4: 103-108.
2. Zheng P, Ding X, Yang J, Chen R. Transverse Vibration of Papermaking Felt. *FIBRES & TEXTILES in Eastern Europe* 2010; 18, 3, 80: 106-108.
3. Kaurov PV, Kokushin NN, Tikhonov AA, Kaurov PV. Mathematical modeling for paper stock drainage at hydrofoils of wire part of paper making machine. *International Journal of Industrial Engineering and Management (IJIEM)* 2011; 1: 27-31.
4. Skoko I, Stepanović J, Petrović V, Stanković M, Stamenković M. Uticaj strukturnih i konstruktivnih parametara formirajućih SSB sita na njihova svojstva. *Savremene tehnologije* 2012; 1: 52-57.
5. Ward IM, Sweeney J. *An introduction to the mechanical properties of solid polymers*. Second Edition, John Wiley and sons, West Sussex, 2004.
6. Banik K. Effect of mold temperature on short and long-term mechanical properties of PBT. *eXPRESS Polymer Letter* 2008; 2: 111–117.
7. Stojiljkovic D, Petrovic V, Djurovic M. Rheological modeling of yarn elongation. *Tekstil* 2007; 9: 551-561.
8. Stepanovic J, Milutinovic Z, Petrovic V, Pavlovic M. Influence of relative density on deformation characteristics of fabrics in plain weave. *Indian Journal of Fibre & Textile Research* 2009; 1: 76-81.
9. Petrović V, Stepanović J, Skoko I, Stankovic M, Stamenkovic M. Analysis of Deformation Characteristics of SSB Forming Sieves. In: *14th Romanian Textiles and Leather Conference*. Sinaia, Romania, 6. – 8. 9. 2012: 158-165.
10. Stepanovic J, Zafirova K, Milutinović Z, Petrović V. Design of fabric breaking characteristics. *Macedonian Journal of Chemistry and Chemichal Engineering* 2007; 1: 45-55.
11. Wu DF, Zhou CX, Fan X, Mao DL, Bian Z. Linear rheological behavior and thermal stability of poly(butylene terephthalate)/epoxy/clay ternary nano composites. *Polymer Degradation and Stability* 2005; 3: 511-520.
12. Chow WS. Tensile and thermal properties of poly-butyleneterephtalate)/ organo-montmorillonite nano composites. *Malaysian Polymer Journal* 2008; 1: 1-13.
13. Hashemi S. Temperature dependence of work of fracture parameters in polybutylene-terephthalate (PBT). *Polymer Engineering & Science* 2000; 6: 1435–1446.
14. Pegoretti A, Gorigato A, Penati A. Tensile mechanical response of polyethylene-clay nano composites. *eXPRESS Polymer Letter* 2007; 1: 123–132.

Received 07.11.2013 Reviewed 26.12.2013